

---

# JOURNAL OF THE AMERICAN CHEMICAL SOCIETY

---

## A Structural Explanation for Enzyme Memory in Nonaqueous Solvents

Hemant P. Yennawar, Neela H. Yennawar, and Gregory K. Farber\*

*Contribution from the Department of Biochemistry & Molecular Biology and Center for Biomolecular Structure and Function, 108 Althouse Laboratory, The Pennsylvania State University, University Park, Pennsylvania 16802*

Received August 11, 1994<sup>⊗</sup>

**Abstract:** Crystalline  $\gamma$ -chymotrypsin soaked in aqueous and nonaqueous solutions containing the inhibitor *N*-acetyl-D-tryptophan has been studied by X-ray crystallographic methods at a resolution of 2.2 Å. This inhibitor has been used to induce "enzyme memory" in chymotrypsin in nonaqueous solvents (Ståhl, M. *et al. J. Am. Chem. Soc.* **1991**, *113*, 9366–9368). The two soak solutions consisted of (a) the inhibitor, water, and 2-propanol and (b) the inhibitor, hexane, and 2-propanol. In the nonaqueous environment, the indole ring of the inhibitor binds in the specificity pocket of the enzyme for L-amino acids and not in a new site as had been suggested by others (Tawaki, S.; Klibanov, A. M. *J. Am. Chem. Soc.* **1992**, *114*, 1882–1884). No inhibitor binding was observed in the aqueous structure even though the concentration of inhibitor was identical to that in the nonaqueous experiment. Five hexane and three 2-propanol molecules were located in the nonaqueous structure. One of the three 2-propanol molecules occupies the P1' binding site. In the aqueous structure one 2-propanol was observed. In both structures, the addition of 2-propanol resulted in a dramatic increase in the number of observed water molecules. The differential binding affinity of *N*-acetyl-D-tryptophan in water and in a nonaqueous environment suggests a molecular explanation for the phenomenon of enzymatic memory.

### Introduction

There has been a great deal of interest in the reactivity of enzymes in nonaqueous media in recent years.<sup>1,2</sup> Enzymes have been reported to be more thermostable in organic solvents,<sup>1</sup> to catalyze reactions which are kinetically or thermodynamically impossible in water,<sup>2–7</sup> and to have dramatically altered substrate

specificity in organic solvents.<sup>8–11</sup> The first two of these novel enzymatic properties in nonaqueous solvents are relatively easy to explain. Thermal inactivation of an enzyme is often due to reaction of the protein with water,<sup>12</sup> and lack of water in the solvent prevents the reaction. Similarly, there is no surprise that chemical equilibrium and/or mechanism changes in different solvents. However, the alteration of substrate specificity is not easy to understand.

One explanation for altered substrate specificity has been

(7) Kasche, V.; Michaelis, G.; Galunsky, B. *Biotechnol. Lett.* **1991**, *13*, 75–80.

(8) Zaks, A.; Klibanov, A. M. *J. Am. Chem. Soc.* **1986**, *108*, 2767–2768.

(9) Zaks, A.; Klibanov, A. M. *J. Biol. Chem.* **1988**, *263*, 3194–3201.

(10) Gololobov, M. Y.; Voyushina, T. L.; Stepanov, V. M.; Adlercreutz, P. *FEBS* **1992**, *307*, 309–312.

(11) Tawaki, S.; Klibanov, A. M. *J. Am. Chem. Soc.* **1992**, *114*, 1882–1884.

(12) Klibanov, A. M. *Adv. Appl. Microbiol.* **1983**, *29*, 1–28.

<sup>⊗</sup> Abstract published in *Advance ACS Abstracts*, December 15, 1994.

(1) Zaks, A.; Klibanov, A. M. *Science* **1984**, *224*, 1249–1251.

(2) Zaks, A.; Klibanov, A. M. *Proc. Natl. Acad. Sci. U.S.A.* **1985**, *82*, 3192–3196.

(3) Homandberg, G. A.; Mattis, J. A.; Laskowski, M., Jr. *Biochemistry* **1978**, *17*, 5220–5227.

(4) Kuhl, P.; Halling, P. J.; Jakubke, H. D. *Tetrahedron Lett.* **1990**, *31*, 5213–5216.

(5) Ståhl, M.; Månsson, M. O.; Mosbach, K. *Biotechnol. Lett.* **1990**, *12*, 161–166.

(6) West, J. B.; Hennen, W. J.; Lalonde, J. L.; Bibbs, J. A.; Zhong, Z.; Meyer, E. F., Jr.; Wong, C. H. *J. Am. Chem. Soc.* **1990**, *112*, 5313–5320.

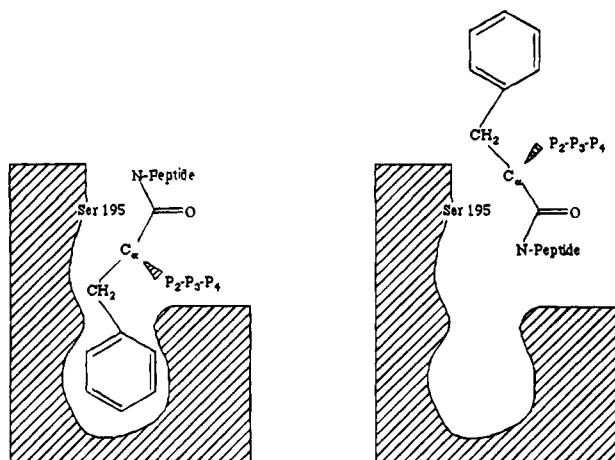


**Figure 1.** Hypothetical solvent induced changes in substrate binding (adapted from a similar figure in reference 11). The cartoon on the left shows how an L-amino acid binds in the active site of chymotrypsin in water. The phenylalanine side chain is bound in the specificity pocket. The cartoon on the right shows how a D-amino acid could bind in the active site when the enzyme is suspended in a nonpolar solvent.

offered by Klibanov and co-workers.<sup>11</sup> They have discovered that the enantioselectivity of aspergillopeptidase B changes with the nature of the solvent. Further, they show that the hydrophobicity of the solvent is correlated with the preference for the D or L enantiomer. They suggest that there are two distinct ways in which the substrate can bind to the enzyme and still be correctly positioned for catalysis (Figure 1). If this suggestion is correct, they suggest that there should be two different ways to bind substrates in serine proteases—one to bind the natural L enantiomer in water and a second to bind the D enantiomer in an organic solvent.

Another aspect of the altered reactivity of enzymes in nonaqueous solvents has been termed ligand induced enzyme memory or bioimprinting. Several groups have shown that when an enzyme is lyophilized from a solution containing a molecule with a particular stereochemistry and is then suspended in an organic solvent, the activity of the enzyme is much higher toward substrates with the same stereochemistry.<sup>5,13,14</sup> The explanation that has been suggested for this behavior is that the enzyme assumes a conformation when the ligand binds which is complementary toward substrates with the same shape. This activated conformation is frozen in place when the enzyme is moved into an organic solvent since mobility is lower in organic solvents than in water.<sup>15</sup> If this suggestion really explains the enzyme memory phenomenon, the binding of an inhibitor with D stereochemistry would cause some structural rearrangement in the active site of a protease. Such a change should be observable in an X-ray crystal structure done in an organic solvent.

The serine protease, chymotrypsin, is an ideal model system to explore the effects of organic solvents on enzymatic catalysis. The chemical and kinetic mechanisms of chymotrypsin have been studied for decades,<sup>16</sup> and a number of structural studies have been reported.<sup>15,17–21</sup> The  $\gamma$ -chymotrypsin form of the enzyme was chosen for the experiments reported here because

it already has a peptide bound in the active site.<sup>15,18–20</sup> The relative populations of inhibitor and peptide in the active site can be used to monitor changes in inhibitor binding affinity in different solvents. Finally, the structure of  $\gamma$ -chymotrypsin in hexane has been reported, and it has been shown that the crystalline enzyme is catalytically active (in both the hydrolysis and synthesis directions) in hexane.<sup>15</sup>

As with aspergillopeptidase B,<sup>11</sup> placing chymotrypsin in organic solvents dramatically alters substrate specificity. Adlercreutz and co-workers have demonstrated that the specificity in the P1' site changes when chymotrypsin is suspended in a solution of acetonitrile, dimethylformamide, and water.<sup>10</sup> Zaks and Klibanov have demonstrated that the specificity in the P1 site also changes when chymotrypsin is suspended in dry octane.<sup>8</sup> Two groups have reported that chymotrypsin catalyzed peptide bond synthesis is possible in organic solvents.<sup>3,7</sup> Some of these reports also show that chymotrypsin can be imprinted to use D-amino acids as a substrate in organic solvents.<sup>5,6,14</sup>

To either find the putative alternate binding pocket for D-amino acids or find conformational differences induced by an inhibitor of unnatural stereochemistry, we solved the crystal structure of  $\gamma$ -chymotrypsin in the presence of *N*-acetyl-D-tryptophan in both hexane and water. Comparison of these structures suggests that the altered substrate specificity of enzymes in organic solvents is due to changes in binding affinity for *N*-acetyl-D-tryptophan rather than the presence of a second specificity pocket in the enzyme. No significant conformational rearrangement was observed in the active site upon the binding of this ligand.

## Experimental Section

**Crystal Preparation.**  $\alpha$ -Chymotrypsin (Sigma, C-4129) was converted to  $\gamma$ -chymotrypsin and crystallized as described previously.<sup>15,21</sup> For the nonaqueous experiment, large (0.5 × 0.5 × 0.8 mm) crystals were transferred to thin-walled quartz capillary tubes (Charles Supper Co.). Capillary tubes of a particular diameter were chosen so that a crystal would wedge roughly halfway down the capillary tube. All aqueous solution was removed from the tube using thin glass pipets and filter paper. The capillary tube was extensively washed with the soak solution and finally submerged in a reservoir containing roughly 50 mL of the soak solution. Since *N*-acetyl-D-tryptophan is sparingly soluble in both hexane and water, it was dissolved in 2-propanol (SIGMA, HPLC grade) to 30 mM concentration. The nonaqueous soak solution was prepared by adding this 2-propanol solution to dry *n*-hexane (HPLC grade from Aldrich) in the ratio of 4:96 v/v. All water was removed from the hexane by storing it over 4Å, 1/8 in., 4–8 mesh molecular sieves. Hexane treated in this way has less than 10 nM of water as determined using a Mettler DL-18 Karl-Fischer titrimer. After 4 days the capillary tube was removed from the reservoir. Pipe cleaner fibers were packed around the crystal to prevent it from moving during data collection. The hexane/2-propanol/inhibitor solution surrounded the crystal and the fibers during data collection. Small volumes of a saturated solution of *N*-acetyl-D-Trp in water were placed on either side of the hexane solution in the capillary tube to prevent hexane evaporation. In most cases, this water layer was not in direct contact with the hexane layer. The capillary tube was sealed with sticky wax and mounted on a goniometer head for data collection.

For the comparative study, the  $\gamma$ -chymotrypsin crystals were grown in the same manner. They were then transferred to capillary tubes. In an effort to dislodge the active site peptide, a solution of 30 mM *p*-nitrophenyl acetate in acetonitrile was added (10% v/v) to the

(13) Russell, A. J.; Klibanov, A. M. *J. Biol. Chem.* **1988**, *262*, 11624–11626.

(14) Ståhl, M.; Jepsson-Wistrand, U.; Månsson, M.-O.; Mosbach, K. *J. Am. Chem. Soc.* **1991**, *113*, 9366–9368.

(15) Yennawar, N. H.; Yennawar, H. P.; Farber, G. K. *Biochemistry* **1994**, *33*, 7326–7336.

(16) Polgar, L. In *Hydrolytic Enzymes*; Neuberger, A., Brocklehurst, K., Eds.; Elsevier Science Publishers B. V. (Biomedical Division): New York, 1987; pp 159–200.

(17) Steitz, T. A.; Shulman, R. G. *Annu. Rev. Biophys. Bioeng.* **1982**, *11*, 419–444.

(18) Dixon, M. M.; Matthews, B. W. *Biochemistry* **1989**, *28*, 7033–7038.

(19) Harel, M.; Su C.-T.; Frolow, F.; Silman, I.; Sussman J. L. *Biochemistry* **1991**, *30*, 5217–5225.

(20) Dixon, M. M.; Brennan, R. G.; Matthews, B. W. *Int. J. Biol. Macromol.* **1991**, *13*, 89–96.

**Table 1.** Data Collection Parameters

	water + 2-propanol	hexane + 2-propanol
space group	P4 <sub>2</sub> 2 <sub>1</sub> 2	P4 <sub>2</sub> 2 <sub>1</sub> 2
unit cell dimenss, Å		
<i>a</i>	69.57	69.59
<i>b</i>	69.59	69.58
<i>c</i>	97.48	97.51
no. of reflcns	15427	15361
resolution, Å	2.2	2.2
no. of crystals	4	4
<i>R</i> <sub>merge</sub> , <sup>a</sup> %	9.7	14.0
isomorphous diff, <sup>b</sup> %		14.2

<sup>a</sup>  $R_{\text{merge}} = \sum |I_j - \bar{I}| / \sum \bar{I}$ , where *j* is a summation over all crystals.

<sup>b</sup> Isomorphous difference =  $\sum |F_{\text{wat}} - F_{\text{hex}}| / \sum F_{\text{wat}}$ , where the summation is over all common reflections.

crystallization buffer (10 mM sodium cacodylate, pH 5.6, 75% saturated ammonium sulfate). We have shown that the crystalline enzyme will hydrolyze *p*-nitrophenyl acetate under these conditions.<sup>15</sup> After 18 h, the capillary tubes containing crystals were transferred to a solution containing 96% crystallization buffer and 4% *N*-acetyl-D-Trp in 2-propanol (30 mM). The crystals soaked in this inhibitor solution for 12 days before being mounted for data collection. Unlike the nonaqueous structure, these crystals were not surrounded by the soaking solution during data collection. They were mounted in the normal way with the soak solution on either side of the crystal, and the capillary tubes were sealed with sticky wax.

**Data Collection.** X-ray data were measured to a nominal resolution of 2.2 Å using a four-circle diffractometer with a rotating anode X-ray source (AFC5R). Radiation was monochromatized using a graphite crystal. Individual background measurements were made for all reflections. Data from different crystals were merged together using a set of 200 common reflections which were measured for each crystal.<sup>22</sup> This common block of reflections was collected at the beginning and at the end of data collection. A radiation damage correction was applied as a function of both time and resolution using these reflections.<sup>23</sup> The hexane data were scaled to the aqueous data set using a single overall scale factor. Programs for data reduction were written in the author's laboratory. Data collection results are summarized in Table 1.

**Structure Refinement.** The starting point for the refinement of the two structures was the high-resolution structure reported by Stoddard *et al.*<sup>21</sup> stripped of all the water molecules and the cinnamate in the active site. This structure was chosen as the starting model to minimize model bias since it does not have a peptide in the active site. Conventional positional and B-factor refinement was done using XPLOR<sup>24</sup> as described previously.<sup>15</sup>

After the initial refinement, the solvent molecules were located using electron density difference maps ( $2F_o - F_c$ ) with a contour level of 1.25 times the standard deviation of the map. Electron density which was consistent with all three types of solvent molecules (water, 2-propanol, and hexane) was observed in these maps (Figure 2 and 3). We also examined maps of the type  $F_{o(\text{nonaqueous})} - F_{o(\text{aqueous})}$  for hexane and 2-propanol densities. Electron density for the nonaqueous solvents was present in these maps, but it was usually not as strong as in the  $2F_o - F_c$  maps. Presumably, this weaker density is due to partial occupancy of water molecules in the hexane or 2-propanol binding sites in the aqueous structure.

Only water molecules with temperature factors less than 25 Å<sup>2</sup> were retained in the model during the initial stages of refinement. In the final stages of refinement this was relaxed to 50 Å<sup>2</sup> because of the persistent reappearance of some of the electron density peaks. In the intermediate steps of the refinement, difference Fourier maps ( $2F_o - F_c$ ) of the nonaqueous structure showed regions of continuous electron density which were just right for the six carbons of a hexane molecule.

(21) Stoddard, B. L.; Bruhnke, J.; Proter, N.; Ringe, D.; Petsko, G. A. *Biochemistry* **1990**, *29*, 4871–4879.

(22) Monahan, J. E.; Schiffer, M.; Schiffer, J. P. *Acta Crystallogr.* **1967**, *22*, 322.

(23) Fletterick, R. J.; Sygusch, J.; Murray, N.; Madsen, N. B.; Johnson, L. N. *J. Mol. Biol.* **1976**, *103*, 1–13.

(24) Brunger, A. T.; Kuriyan, J.; Karplus, M. *Science* **1987**, *235*, 458–460.

Our confidence in these hexane positions stemmed from the fact that no such density was ever seen in either the water/2-propanol structure or the native structure reported previously.<sup>15</sup> The hexane molecules were built into the map using O,<sup>25</sup> tested for short contacts, and added to the preliminary model. Only those hexanes which had reasonable temperature factors were retained. Five hexane molecules refined successfully. Similarly, regions of density suitable for 2-propanol molecules were noticed during the course of refinement. The trigonal pyramidal geometry of the 2-propanol density could not be satisfactorily modeled as a cluster of waters. During the process of refinement and model building a total of four 2-propanol molecules were identified. However, only three of these molecules refined successfully. During subsequent refinement rounds, the temperature factors for the fourth 2-propanol became large and the electron density disintegrated.

Once the solvent modeling for both structures was completed, simulated annealing omit maps were computed using XPLOR to examine both the active site and the organic solvent sites. Such omit maps minimize the model bias in the electron density.<sup>26</sup> In the active site, residues in a 8.0 Å sphere centered at Ser 195 (of the catalytic triad) were omitted from the model. An 8.0 Å sphere was also used to examine the organic solvent sites (Figure 3). Atoms in the shell from 8 to 11 Å were harmonically restrained to prevent them from moving into the omitted region. Simulated annealing was carried out beginning at an initial temperature of 1600 K with cooling in increments of 50 K to a final temperature of 300 K. The active site density in the aqueous structure was similar to that found in the normal crystallization buffer.<sup>15</sup> The density was appropriate for a tetrapeptide (Pro-Val-Gly-Tyr) bound in the P4–P1 subsites. All of the organic solvents returned with reasonable density in these omit maps.

In the hexane/2-propanol structure the density was quite different in the active site than in the aqueous structure (Figure 4). The density in the specificity pocket indicated the presence of a side chain which was larger than the usual Tyr of the active site peptide. In this density we modeled the inhibitor molecule *N*-acetyl-D-tryptophan (*N*-acetyl-D-Trp). There was also some weak density in the P4–P2 subsites. This density was modeled as the active site peptide sequence Pro-Val-Gly. The inhibitor and the peptide were both refined at 0.5 occupancy. A summary of the refinement results is in Table 2.

The coordinates for the two structures with 2-propanol and *N*-acetyl-D-Trp have been sent to the Brookhaven Protein Data Bank and have been assigned the names 1GBH for the hexane structure and 1GBA for the aqueous structure.

## Discussion

**Active Site.** The active site of chymotrypsin can be divided into two different regions. Ser 195 is at the center of the region where catalysis occurs. The residues of the catalytic triad (Ser 195, His 57, Asp 102) are arranged so that the OG of Ser 195 is positioned to attack the carbonyl carbon of the substrate. The oxygen of the substrate carbonyl is bound in the oxyanion hole created by the backbone nitrogens from residues 193 and 195. The other region of the active site determines the substrate specificity of the enzyme. Chymotrypsin has a series of amino acid binding sites which are designated P1 for the amino acid side chain adjacent the scissile bond, P2 for the next side chain, and so on.<sup>27</sup> For  $\gamma$ -chymotrypsin in the normal crystallization buffer, electron density for a tetrapeptide can be observed in the P1 through P4 subsites.<sup>15,18–20</sup> In water, chymotrypsin prefers aromatic amino acids in the P1 position. This specificity is achieved by binding of the aromatic side chain into a groove formed by a number of amino acids. Met 192 is close to the bottom of this groove.

(25) Jones, T. A.; Zou, J. Y.; Cowan, S. W.; Kjeldgaard, M. *Acta Crystallogr.* **1991**, *A47*, 110–119.

(26) Hodel, A.; Kim, S. H.; Brunger, A. T. *Acta Crystallogr.* **1992**, *A48*, 851–858.

(27) Schechter, I.; Berger, A. *Biochem. Biophys. Res. Commun.* **1967**, *27*, 157–162.

(28) Henderson, R. *J. Mol. Biol.* **1970**, *54*, 341–354.

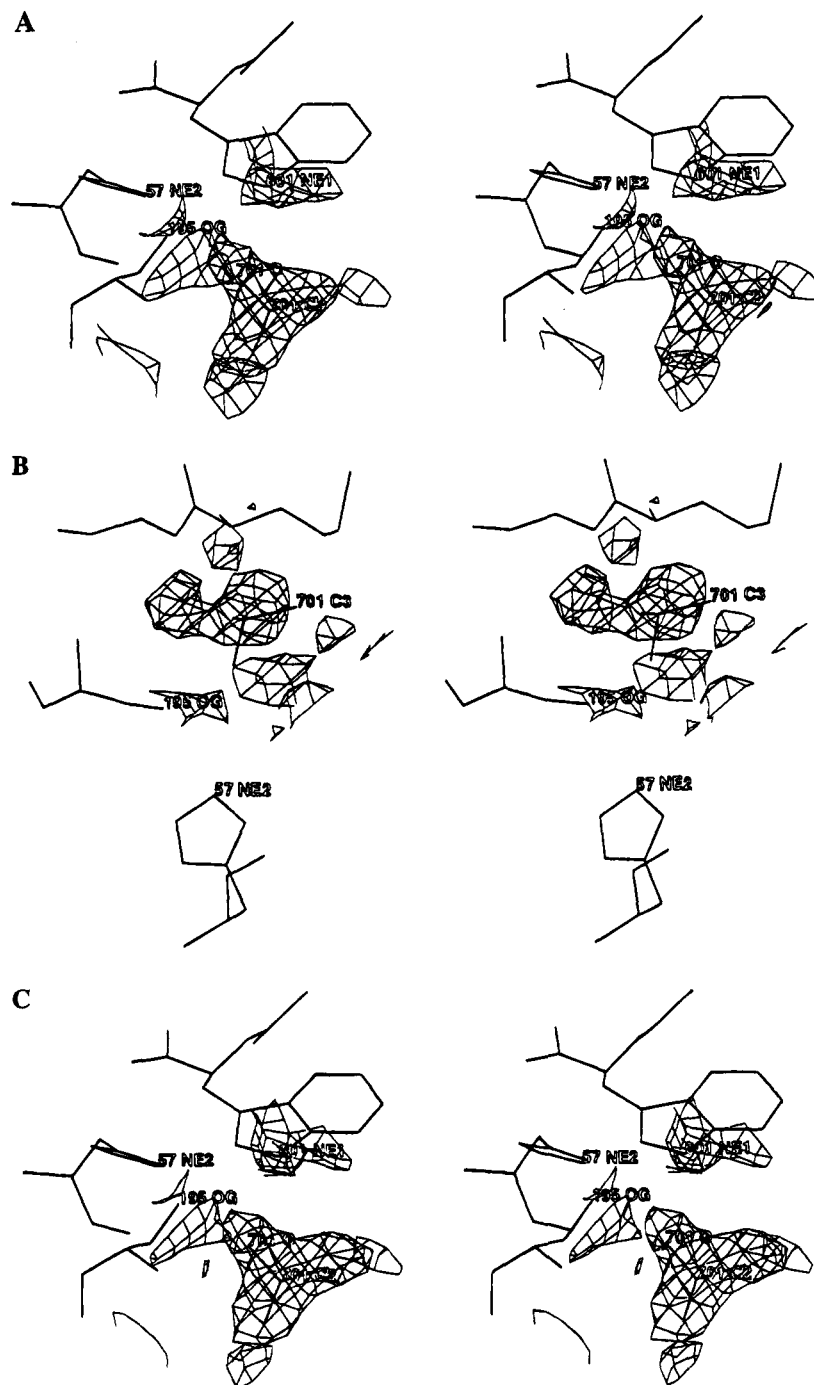


**Figure 2.** Electron density for a typical 2-propanol molecule. This molecule is located in the P1' site of the hexane + 2-propanol structure. All maps are contoured at  $1.25 \sigma$ , and the same final refined coordinates are used in all three maps. Part A shows a map with Fourier coefficients  $2F_o - F_c$ . The  $F_c$  and the phases were derived from a refined model of chymotrypsin with no solvent and no inhibitor in the active site. Part B shows a map with Fourier coefficients  $F_{o(\text{hexane}+2\text{-propanol})} - F_{o(\text{water}+2\text{-propanol})}$ . The phases were the same as those used for Part A. The density for the 2-propanol is less well defined in this map due to the information about the water structure in the water + 2-propanol data. Part C shows the final  $2F_o - F_c$  map with phases derived from the final model (including the solvent).

In the water/2-propanol structure with *N*-acetyl-D-Trp in the solution, the active site is similar to that observed previously (Figure 5).<sup>15,18-20</sup> The Tyr of the active site peptide is bound in the specificity pocket. There is no hint of any density for the inhibitor. Ser 195 is close to the carbonyl carbon, but unlike earlier structures<sup>15</sup> the density for the active site peptide is broken at the catalytic serine rather than continuous. Because of this difference, the peptide was modeled as the E-peptide complex rather than the acyl enzyme intermediate.

Five intermediates are thought to exist in the reaction catalyzed by chymotrypsin.<sup>16</sup> They are the E·S complex, the

first tetrahedral intermediate with Ser 195 attacking the carbonyl carbon, the acyl enzyme intermediate with the substrate covalently bound to Ser 195, the second tetrahedral intermediate with water attacking the acyl enzyme, and the E·P complex. Crystal structures are now available for four of these five structures. The present work provides the structure of the E·P complex. We have reported the structure of the first tetrahedral intermediate by transferring crystals of chymotrypsin to hexane under conditions where the reaction could occur in the synthetic direction.<sup>15</sup> The acyl enzyme intermediate structure has been known for some time.<sup>18-20</sup> The approach to the second

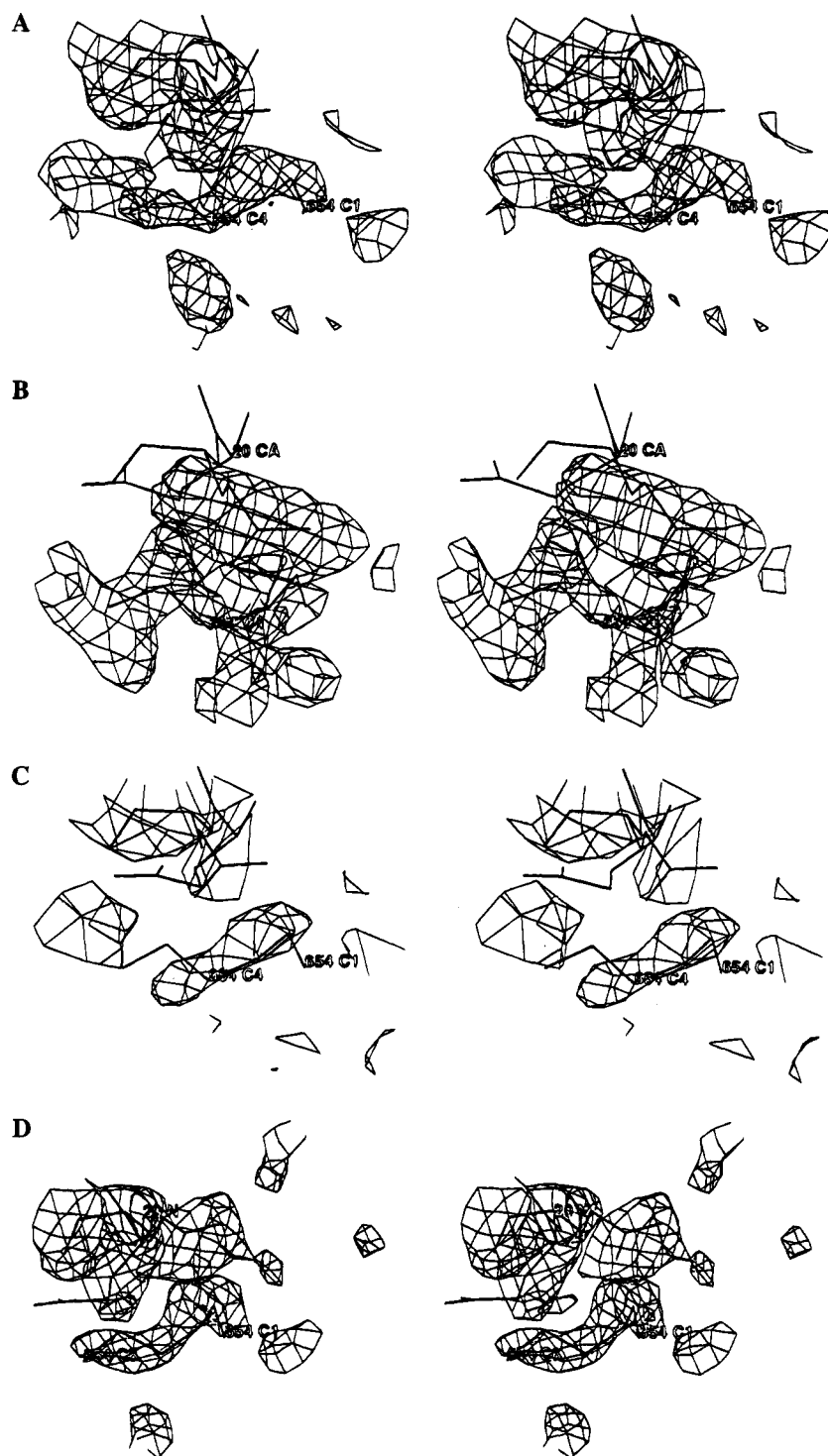


**Figure 3.** Electron density for a typical hexane molecule (Hex 654). All maps are contoured at  $1.25 \sigma$ , and the same final refined coordinates are superimposed in all four maps. Part A shows a map with Fourier coefficients  $2F_o - F_c$ . The  $F_c$  and the phases were derived from a refined model of chymotrypsin with no solvent and no inhibitor in the active site. Part B shows a map with Fourier coefficients  $F_o(\text{hexane}+2\text{-propanol}) - F_o(\text{water}+2\text{-propanol})$ . The phases were the same as those used for Part A. Part C shows the density from a simulated annealing omit map. Part D shows the final  $2F_o - F_c$  map with phases derived from the final model (including the solvent).

tetrahedral intermediate was observed using the Laue method of data collection following a pH jump with trypsin.<sup>29</sup> In that structure, the hydrolytic water was observed moving into position to attack the carbonyl carbon. Only the E•S complex remains to be observed to finish the crystallographic movie of serine protease catalysis.

In the hexane/2-propanol structure, the active site region is quite different since the *N*-acetyl-D-tryptophan has partially

(29) Singer, P. T.; Smalås, A.; Carty, R. P.; Mangel, W. F.; Sweet, R. M. *Science* **1993**, *259*, 669–673.

replaced the active site peptide (Figure 4). There is weak density for the peptide in the P2, P3, and P4 subsites. However, the electron density for the peptide in the P1 subsite is quite different from the density which we observe in all of our other  $\gamma$ -chymotrypsin structures in both hexane and water.<sup>15</sup> The electron density in the specificity pocket which was occupied by the Tyr side chain of the tetrapeptide is much bulkier and extends itself in a new direction. This density is suitable for a molecule of *N*-acetyl-D-Trp with the Trp side chain occupying

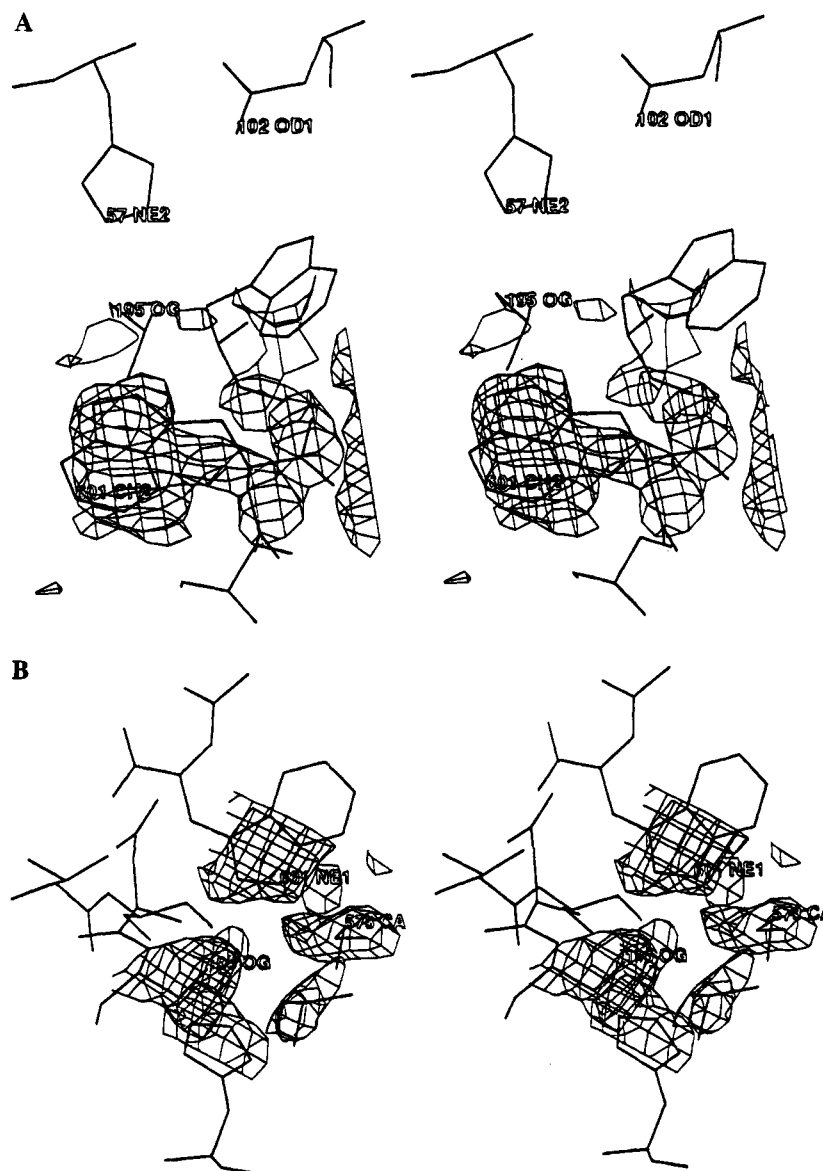


**Figure 4.** The active site in the hexane/2-propanol structure. For both maps, the density comes from a  $2F_o - F_c$  map with  $F_c$  and phases derived from a model without the inhibitor or solvent. The contour level is  $1.25\sigma$ . (A) A view of the inhibitor. Ser 195, His 57, and Asp 102 are all labeled. Clearly, there is too much density in the specificity pocket for just the tyrosine side chain of the peptide. The inhibitor accounts for the density reasonably well, but the match is not perfect. This discrepancy can be accounted for by the partial occupancy of the Tyr of the active site peptide. (B) Density for the amino acid in the P2 position of the active site.

the specificity pocket and the peptide backbone extending in a new direction (Figure 4). Since there is weak density for the peptide in the P2, P3, and P4 subsites, some of the density in the specificity pocket must be due to the Tyr in the P1 subsite. However, Figure 4 clearly shows additional density which is fit well by *N*-acetyl-D-Trp. Under the soaking conditions of the nonaqueous experiment, the inhibitor has displaced most, but not all, of the original active site peptide.

The indole ring of the inhibitor is bound in exactly the same site as the tyrosine side chain of the peptide, and the six-membered rings of the two structures overlap (Figures 4 and 5). The only significant change in the specificity pocket between the two structures involves Met 192. The terminal methyl of the side chain in the nonaqueous structure has swung away from its position in the native structure to make room for the bulkier Trp side chain.

Unlike the cartoon shown in Figure 1, the carbonyl carbon of the inhibitor is 6.8 Å away from Ser 195. In this new orientation, the carbonyl is close to Ser 189 (Figure 6). If the

inhibitor backbone had been any larger, it could not have rotated into this position. Keeping the tryptophan ring stationary and changing only torsion angles, it is possible to move the carbonyl carbon close to Ser 195 (3.1 Å). This makes us believe that the inhibitor *N*-acetyl-D-Trp is binding in the same manner as a true substrate with D stereochemistry would bind.

**Hexane and 2-Propanol Locations.** The final model for the hexane/2-propanol structure has five hexane, three 2-propanol, and 307 water molecules. In one of our earlier experiments with  $\gamma$ -chymotrypsin crystals soaked in hexane alone, seven enzyme bound hexane molecules were found.<sup>15</sup> In the present structure three hexane molecules Hex 651, Hex 652, and Hex 653 are located in the sites occupied by hexanes in the earlier structure while the remaining two, Hex 654 and Hex 655, occupy new sites.

Hex 651 replaces two water molecules found in both the native<sup>15</sup> and the water/2-propanol structures. It is surrounded by one water molecule and residues Thr 144, Glu 156, Arg 145, and Pro 152. As we have seen previously, the side chains of

Table 2. Refinement Statistics<sup>a</sup>

	water + 2-propanol	hexane + 2-propanol
no. of water molecules	173	307
no. of 2-propanol molecules	1	3
no. of hexane molecules		5
<i>R</i> factor, %	16.4	15.2
$\delta$ bond, <sup>b</sup> Å	0.011	0.010
$\delta$ angle, <sup>b</sup> deg	1.631	1.606
mean <i>B</i> -factor, Å <sup>2</sup>		
protein	3.49	5.66
water	19.10	24.01
hexanes		14.42
2-propanol	15.66	8.55
active site peptide	23.74	7.45 <sup>c</sup>
<i>N</i> -acetyl-D-Trp		8.65 <sup>c</sup>

<sup>a</sup>The number of heavy atoms in the aqueous structure including the active site peptide is 1766. For positional refinement, reflections with  $F > 2.0\sigma(F)$  and within the resolution range 10–2.2 Å were used. For *B*-factor refinement, reflections with  $F > 2.0\sigma(F)$  and within 5–2.2 Å resolution range were included in calculations. The final *R*-factor was calculated using the 5–2.2 Å shell of data. The unit cell parameters used for both structures were  $a = b = 69.60$  Å,  $c = 97.51$  Å. <sup>b</sup>Root-mean-square discrepancies from ideal values. <sup>c</sup>The peptide was modeled into the weak density on the P2, P3, and P4 subsites. Only *N*-acetyl-D-Trp was modeled in the P1 subsite.

surface residues often have new conformations in hexane.<sup>15</sup> In this case, CG of Arg 145 moves toward Hex 651.

Hex 652 lies on the surface of the enzyme molecule and is situated close to a 2-fold symmetry axis. Consequently it has its symmetry related counterpart as its neighbor. The hexane pair is surrounded by Val 188 and Leu 10 from the two protein molecules. In addition, there are several water molecules surrounding the hexanes.

Hex 653 is shifted three bond lengths from Hex 407 of the structure reported earlier.<sup>15</sup> It replaces two water molecules which were observed in both of the aqueous structures we have studied. C6 of Hex 653 is surrounded by five water molecules forming an open ring clathrate structure. This water ring is partially sandwiched between 653 and 655 hexane molecules. Other neighbors for Hex 653 are Cys 1, Gly 2, and Val 3. A closed ring clathrate similar to this has been observed around one of the hexane molecules in our earlier structure.<sup>15</sup>

Both of the new hexane positions replace water molecules. Hex 654 is on the surface of the enzyme. Its nearest neighbors are Glu 20 and Glu 21. The nearest neighbor for Hex 655 is also a glutamic acid. Glu 49 projects towards the hexane unlike in the water/2-propanol structure where it is oriented in a different manner. This hexane is mainly surrounded by a cylindrical wall of waters which form hydrogen bonds with each other; the radius of the cylinder is 4 Å.

In addition to five hexane molecules, three 2-propanol molecules are observed in the nonaqueous structure. One of the three 2-propanol molecules, Iso 701, binds the P1' site of the enzyme displacing three water molecules including the Henderson water.<sup>28,29</sup> This site is close to the catalytically active Ser 195. The hydroxyl group forms a hydrogen bond with the carbonyl oxygen of Ala 573 (from the peptide in the active site) by donating a proton and accepts a hydrogen bond from NE2 of His 57. In the water/2-propanol structure there is no 2-propanol at the site of Iso 701.

The second 2-propanol molecule, Iso 702, is very close to Pro 501 of the peptide which is bound in the P4 subsite of chymotrypsin.<sup>15</sup> It replaces one water which was observed in the same location in the original hexane structure.<sup>15</sup> Its hydroxyl group interacts with the OG and N atoms of Ser 218. A 2-propanol molecule in this position is also observed in the water/2-propanol structure.

The third 2-propanol is on the surface of the protein and replaces two waters observed in the native structure. It forms a hydrogen bond with the carbonyl oxygen of Ala 56. Other neighbors are Gly 59, Val 60, Val 88, and Lys 90. This site is not occupied by 2-propanol in the water/2-propanol structure.

Although the non-aqueous soak solution contained 96% hexane and just 4% 2-propanol (14:1 mole ratio) we observe three molecules of 2-propanol for every five molecules of hexane entering the crystal lattice. The combination of hydrophobic and hydrophilic surfaces of the 2-propanol molecule combined with its small size seems to aid its diffusion into the crystal lattice. This is supported by the fact that crystals of chymotrypsin soaked in pure 2-propanol shatter quickly.

**Water Structure.** We have located and refined 307 water molecules in the nonaqueous structure and 173 water molecules in the aqueous structure. Both these numbers are roughly double the number of waters observed in the comparable structures with no 2-propanol or inhibitor<sup>15</sup> (Table 3, Figure 7). In those earlier structures we observed 130 water molecules in the hexane structure and 97 water molecules in the native structure. The waters were built by the same people in the laboratory and refined in the same manner in all four structures. The crystals were grown and treated in the same way for these structures and the data collection was identical. For these reasons, we believe that the dramatic increase in the number of waters is not an artifact.

The large number of water molecules confirms predictions made by Timasheff using the thermodynamics of weak binding systems.<sup>30</sup> He reported that when proteins are placed in solution with weak binding molecules such as urea (or in this case 2-propanol), preferential hydration can occur around the protein. The additional waters that we see are bound primarily on the surface of the protein. Thirty six waters are conserved (within 1.5 Å in each structure) in all four structures. Most of these waters are found in the interior of the protein. In addition to the 36 conserved waters, the native structure (in water) has 61 additional waters. Many of these additional waters are also in the interior of the protein, but some are on the surface. In the structure with 96% water and 4% 2-propanol, 76 more waters were observed than in the native structure. These waters are found on the surface of the protein (Figure 7A).

A similar change occurs between the hexane and hexane/2-propanol structures. The waters in the hexane structure are similar in number and in distribution to the waters in the structure with 96% water + 4% 2-propanol. In the structure with hexane + 2-propanol, all of the additional waters are on the surface. Some of the additional waters are in the regions between symmetry related molecules, but many of these additional waters are in the solvent channels quite far from any protein atoms.

The increase in the number of water molecules when 2-propanol is added is consistent with the changes which have occurred in the active site in the aqueous structure. The acyl enzyme intermediate is stable in crystals of  $\gamma$ -chymotrypsin stored in aqueous solution at low pH.<sup>20</sup> When 4% 2-propanol is added to this solution, the number of observed water molecules doubles. This increase in effective water concentration apparently shifts the equilibrium between the acyl enzyme intermediate and the enzyme-peptide complex in which the tetrapeptide is bound noncovalently to the active site (after hydrolysis of the bond to the serine).

**Long-Range Effects of Hydrophobic Environment.** The crystals of  $\gamma$ -chymotrypsin with the inhibitor soaked in both the nonaqueous and the aqueous medium both diffracted to 2.2 Å resolution. The enzyme structures show no major structural

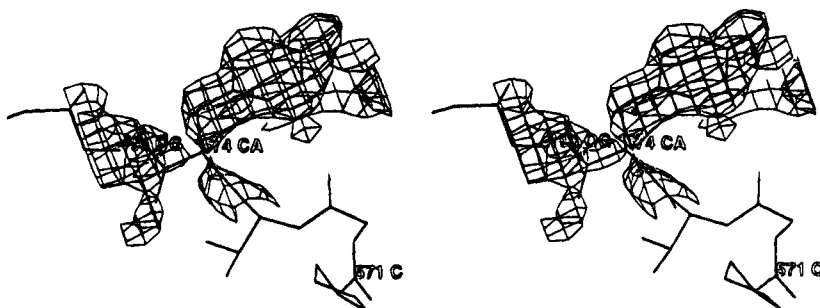


**Figure 5.** The active site of the water + 2-propanol structure. The map was calculated with Fourier coefficients  $2F_o - F_c$ . The  $F_c$  and the phases were derived from a refined model of chymotrypsin with no solvent and no peptide in the active site. Density for Ser 195 of the catalytic triad is shown in this figure along with the Tyr of the active site peptide. The coordinates for the rest of the peptide bound in the active site are also shown although the density for these residues is not shown for clarity. The density between the OG of Ser 195 and the carbonyl carbon of the peptide is continuous, but the density between the carbonyl carbon and the  $\alpha$  carbon of the peptide is broken. Our earlier structures in crystallization buffer with no 2-propanol showed continuous density in this region.<sup>15</sup>

**Table 3.** Comparison of the Structures<sup>a</sup>

RMS Deviation of Backbone Atoms			
	hexane	water + 2-propanol	hexane + 2-propanol
native	0.5	0.2	0.5
hexane		0.6	0.5
water + 2-propanol			0.5
RMS Deviation of Sidechain Atoms			
	hexane	water + 2-propanol	hexane + 2-propanol
native	0.5	1.0	1.0
hexane		1.0	1.1
water + 2-propanol			0.4
Conserved Water Molecules (within 1.5 Å in two structures)			
	hexane	water + 2-propanol	hexane + 2-propanol
native	57	65	64
hexane		54	58
water + 2-propanol			82

<sup>a</sup> The native and hexane structures have been described elsewhere.<sup>15</sup> The native structure has 97 waters, and the hexane structure has 130 waters and 7 hexane molecules. The water + 2-propanol and hexane + 2-propanol structures are described in this work.

change from the known  $\gamma$ -chymotrypsin structures. The average root-mean-square (rms) deviation between backbone atoms for the two structures is 0.499 Å.

Although the hydrophobic environment does not induce any major structural change, the side chains of some residues reorient themselves. The most notable are rearrangement of Arg 154, Lys 93, and Lys 79 side chains. When compared with the native (aqueous) structure,<sup>15</sup> the average rms deviations for each of these side chains are 4.72, 3.82, and 3.47 Å. There are eight other side chains whose average rms deviation values range between 2 and 3 Å. The large side chain rearrangements have two different causes. In some cases, the side chain forms stronger intraprotein interactions. This is similar to the behavior seen earlier<sup>15</sup> which we have attributed to stronger hydrogen bonds and electrostatic interactions in nonaqueous solvents. In other cases, the side chains make hydrogen bonds with the new waters which are immobilized by the addition of 2-propanol.

## Conclusion

With this and the earlier experiments<sup>15</sup> we have found that the chymotrypsin crystals are stable in hexane without any special treatment (e.g. glutaraldehyde cross-linking). The overall conformation of chymotrypsin does not change in a nonaqueous environment. However, changes in side chain positions do

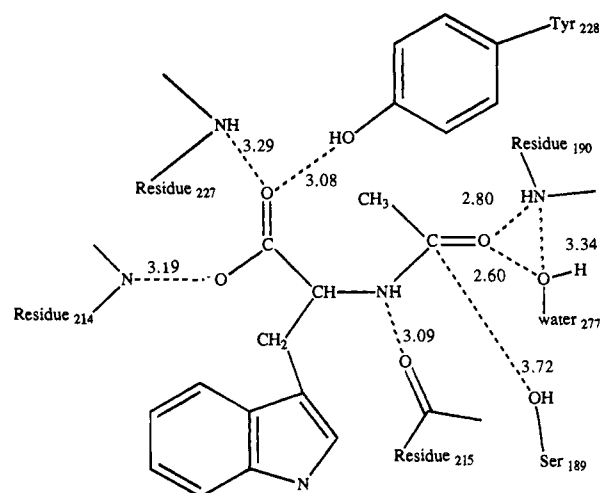


**Figure 6.** A cartoon of the active site of the hexane + 2-propanol structure with *N*-acetyl-D-Trp bound. All of the hydrogen bond interactions with the backbone of the inhibitor are shown. There are many interactions made with the tryptophan ring of the inhibitor which are not explicitly shown in this figure.

occur, and these changes are similar in magnitude to those observed in site-specific mutants. It is likely that these changes are responsible for the altered substrate specificity in the P1 and P1' when chymotrypsin is placed in organic solvents.

The protein atoms of chymotrypsin undergo small, but interesting, changes when placed in an organic solvent. The structure of the solvent is much more dramatically affected. The number of observed water molecules doubles when 4% 2-propanol is added to either water or hexane. Results with other proteins and other additives in this laboratory show that 2-propanol is not unique in causing a dramatic increase in the number of waters which can be observed. This new technique makes it possible to adjust the effective water concentration in the protein crystal. In the case of chymotrypsin, we have been able to trap two intermediates by adjusting the water concentration. In hexane, where the effective concentration of water is low, the tetrahedral intermediate was observed.<sup>15</sup> In a solvent with a high effective water concentration (the 4% 2-propanol structure reported in this work), the acyl enzyme intermediate has been converted into the enzyme-product intermediate.

In the hexane/2-propanol mixture *N*-acetyl-D-Trp does bind in the active site. For the crystals soaked in water/2-propanol, the interaction of the inhibitor with the enzyme is not strong enough to displace the active site peptide even though the



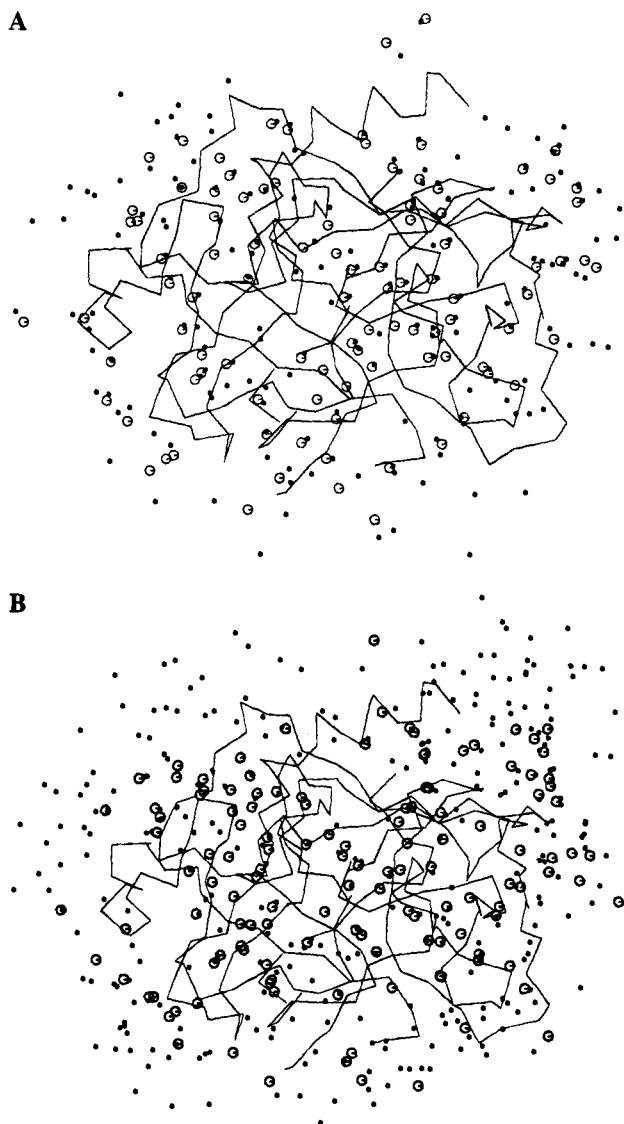


**Figure 7.** The water structure surrounding chymotrypsin. The  $\alpha$ -carbon backbone is shown in both parts. In A the waters from the structure done in normal crystallization buffer<sup>15</sup> are shown as open circles. The waters from the water + 2-propanol structure are shown in filled circles. The majority of the additional waters observed when 2-propanol is added are on the surface of the protein. In B the waters observed when the crystals were soaked in hexane<sup>15</sup> are shown as open circles. The waters observed in the 96% hexane + 4% 2-propanol structure are shown as closed circles. Many of the additional waters observed in the hexane + 2-propanol structure are quite far from the surface of the protein.

soaking time was three times longer than in the hexane/2-propanol structure. Unlike the theory advanced for aspergillopeptidase B,<sup>11</sup> we find no evidence for a second way to bind D amino acids in organic solvents. Chymotrypsin binds both D- and L-amino acids in the same specificity pocket in either water or hexane. However, the binding affinity does change between the two solvents. Since we do not have independent measurements of the binding constants for the inhibitor and the peptide in both solvents, our results can be explained in two ways. Either *N*-acetyl-D-Trp binds better in hexane than in the crystallization buffer or the active site peptide binds more tightly in the aqueous crystallization buffer than in hexane. If the latter explanation were correct, we would have expected to see reduced occupancy for the peptide in our previous structure of  $\gamma$ -chymotrypsin in hexane.<sup>15</sup> No decrease in occupancy was observed when that structure was compared to the structure in the normal aqueous crystallization buffer. So, we conclude that *N*-acetyl-D-Trp does bind more tightly to the active site when the protein is in hexane.

This differential binding could explain the phenomenon of enzymatic memory which has been reported for enzymes in nonaqueous solvents.<sup>13</sup> For chymotrypsin, it has been reported that if the enzyme is lyophilized in the presence of *N*-acetyl-D-Trp and then resuspended in an organic solvent, it is able to accept D-amino acids as substrates in the synthetic direction.<sup>5,14</sup> Enzyme which has been lyophilized with either no ligand or *N*-acetyl-L-Trp shows greatly reduced activity toward D-amino acid substrates. Our structures show that *N*-acetyl-D-Trp binds with similar affinity to a peptide in the active site in a nonaqueous solvent. It seems reasonable to suggest that *N*-acetyl-L-Trp would bind with even higher affinity. The lack of enzymatic activity when chymotrypsin is lyophilized with *N*-acetyl-L-Trp could simply be due to tight binding of this inhibitor in the organic solvent. The low enzymatic activity found when chymotrypsin is lyophilized with no ligand suggests that *N*-acetyl-D-Trp acts as a lyoprotectant.<sup>31</sup> Our structures suggest that the observed changes in  $V_{\max}$  which have been ascribed to imprinting are really due to changes in the active enzyme concentration (due to both inhibition and lyoprotection by the "imprinting" molecule) rather than true changes in  $k_{\text{cat}}$ .

**Acknowledgment.** We thank C. Robert Matthews and Ken Merz for encouragement and many helpful discussions. This work was supported by the Office of Naval Research.

JA9426655

(31) Dabulis, K.; Klibanov, A. M. *Biotechnol. Bioeng.* **1993**, *41*, 566–571.